EPJ Web of Conferences **109**, 05001 (2016)
DOI: 10.1051/epjconf/201610905001

Projected shell model for Gamow-Teller transitions in heavy, deformed nuclei

Long-Jun Wang[1], Yang Sun[1,2,3,4,a], Zao-Chun Gao[3,4], and Surja Kiran Ghorui[1]

[1] *Department of Physics and Astronomy, Shanghai Jiao Tong University, Shanghai 200240, China*
[2] *Collaborative Innovation Center of IFSA (CICIFSA), Shanghai Jiao Tong University, Shanghai 200240, China*
[3] *China Institute of Atomic Energy, P.O. Box 275(18), Beijing 102413, China*
[4] *State Key Laboratory of Theoretical Physics, Institute of Theoretical Physics, Chinese Academy of Sciences, Beijing 100190, China*

Abstract. Calculations of Gamow-Teller (GT) transition rates for heavy, deformed nuclei, which are useful input for nuclear astrophysics studies, are usually done with the quasiparticle random-phase approximation. We propose a shell-model method by applying the Projected Shell Model (PSM) based on deformed bases. With this method, it is possible to perform a state-by-state calculation for nuclear matrix elements for β-decay and electron-capture in heavy nuclei. Taking β^- decay from ^{168}Dy to ^{168}Ho as an example, we show that the known experimental B(GT) from the ground state of the mother nucleus to the low-lying states of the daughter nucleus could be well described. Moreover, strong transitions to high-lying states are predicted to occur, which may considerably enhance the total decay rates once these nuclei are exposed to hot stellar environments.

1 Introduction

The knowledge on weak interaction processes is important not only for nuclear and particle physics, but also for nuclear astrophysics [1–5]. For example, to constrain the neutrino mass from the neutrinoless double beta decay experiments, one needs to calculate nuclear matrix elements of the Gamow-Teller (GT) transition strengths, B(GT), between the ground states of the mother and daughter nucleus as accurately as possible [6, 7]. On the other hand, β-decay rates are indispensable nuclear inputs for understanding the nucleosynthesis processes such as the s-process, the r-process, and the rp-process. It has been suggested that information of the nuclei involved in these processes plays a crucial role for determination of the GT transitions [5]. Moreover, B(GT) of electron-capture reaction for highly-excited states of medium-heavy and heavy nuclei are an important ingredient to model the late evolution of stars and the core-collapse supernovae [5, 8, 9, 12].

GT transitions can be studied by two kind of experimental methods, the β-decay experiments and the Charge-Exchange (CE) reactions [13]. The β-decay experiments have a simple physical mechanism and can provide high energy-resolution data, but the excitation energy of the study is limited by the Q-value which varies from less than one MeV close to the stability line to about 10 MeV when

[a] e-mail: sunyang@sjtu.edu.cn

Article available at http://www.epj-conferences.org or http://dx.doi.org/10.1051/epjconf/201610905001

going far from the stability. The other limitation of β-decay experiments is that most nuclei undergo either β^+ or β^- decay, but not both. For example, most neutron-rich nuclei could only undergo β^- decay, while the electron-captures of neutron-rich nuclei in the β^+ direction are crucial for core-collapse supernova modeling. On the other hand, the charge-exchange reactions, which are mediated by the strong force, could be used for extracting B(GT) since they connect the same initial and final states as β-decay [14]. CE reactions could make transitions both in the β^- direction, such as the $(p,\ n)$, $(^3\mathrm{He},\ t)$ and $(^6\mathrm{Li},\ ^6\mathrm{He})$ reactions, and in the β^+ direction, such as the $(n,\ p)$, $(d,\ ^2\mathrm{He})$, $(t,\ ^3\mathrm{He})$ and $(^7\mathrm{Li},\ ^7\mathrm{Be})$ reactions. Another advantage of using CE to probe GT transition strengths is that it allows access to higher excitation energy since it is not limited by the Q-value. However, taking the CE reactions in the β^+ direction as example, the $(n,\ p)$ reaction that has the simplest reaction mechanism suffers from poor energy-resolution ($\sim$1 MeV). The $(d,\ ^2\mathrm{He})$ reaction can reach a resolution of 100-200 keV, but the reaction mechanism is complex and only a few examples from early experiments were reported [15, 16]. Although the reaction mechanism of the $(t,\ ^3\mathrm{He})$ reaction with resolution of 250-400 keV has been well studied, it is still impossible to measure accurately GT strengths of all states for many nuclei that are involved in the nuclear networks. Therefore, despite of the experimental advances, one has to rely heavily on the theoretically-calculated GT strength distributions.

Theoretically, two kinds of nuclear models are most commonly used for calculations of GT transition rates: the quasiparticle random-phase approximation (QRPA) and the (spherical) shell model (SM) [5, 9, 17]. The QRPA begins with some (self-consistent) mean-field models, and the residual correlations among nucleons are considered by one-particle-one-hole ($1p-1h$) excitations within the model space. In QRPA, however, the calculated nuclear states are usually not angular-momentum states and the higher-order correlations among nucleons are neglected. On the other hand, the shell model, which diagonalizes the matrix of an effective Hamiltonian in a chosen model space spanned by the Slater determinants of valence nucleons, can treat explicitly two-body correlations among them. It has been suggested that the shell model is the preferable method for GT transition calculations for the nuclear astrophysical purpose [5, 18, 19]. In fact, successful description of nuclear ground states, energy spectra at moderate excitations, and electromagnetic and GT transitions among these states, could be obtained by the shell-model diagonalization method. For example, the nuclear wave functions in the full *sd*-shell model space obtained by Wildenthal and Brown were applied to calculate the GT transition rates for the *sd*-shell nuclei [20–22]. Later, Langanke and Martínez-Pinedo made the shell-model GT rates available also for the pf-shell nuclei [23].

Despite the great success of the shell model description in spectra and transitions for light and some medium-heavy nuclei (the nuclei up to the mass-60 region), some problems still exist in modern shell-model calculations. First, in most cases, the model space is spanned by a single harmonic-oscillator shell, which means that it can not calculate forbidden transitions since such transitions occur between different harmonic-oscillator shells with different parities. Second, it is well known that the shell model suffers from the unavoidable problem of dimension explosion when treating heavier nuclei. This unfortunately excludes shell-model applications to the heavy, deformed mass regions. Finally, shell-model calculations for the GT transitions for highly-excited nuclear states have usually been applied with an assumption based on the Brink-Axel hypothesis [10, 11], which has however been found recently to be invalid at low and moderate initial excitation energies [12].

In the long history of the nuclear shell-model development, tremendous effort has been devoted to extending the shell-model capacity from its traditional territory to heavier shells. As it is impossible to treat an arbitrarily large nuclear system in a spherical shell model framework, one is compelled to seek judicious schemes to deal with large nuclear systems. The central issue has been the shell-model truncation. There are many different ways of truncating a shell-model space. While in principle, it does not matter how to prepare a model basis, it is crucial in practice to use the most efficient one.

In this regard, we recognize the fact that except for a few lying in the vicinity of shell closures, most nuclei in the nuclear chart are deformed. This naturally suggests for shell model calculations to use a deformed basis to incorporate the physics in large systems. Using a deformed basis to perform shell-model calculations is the philosophy that the Projected Shell Model (PSM) follows [24, 25].

The PSM was established in the 1990's [24] and has been successfully applied to descriptions for low-lying spectra and the corresponding electromagnetic transitions, for example, for superdeformed nuclei [26], superheavy nuclei [27], proton-rich nuclei [28], and neutron-rich nuclei [29–31]. To compare with methods in the QRPA approach, the PSM has well-defined wave functions in the laboratory framework with good angular momentum. To compare with conventional spherical shell models, the PSM does not have the limitation in the size of nuclei to be applied. An initial attempt for the PSM to calculate GT transitions was reported in Ref. [32]. The work has recently been extended to odd-mass systems, which will be reported elsewhere [33]. Systematical applications of the method to the actual problems mentioned above have been planned. Before a detailed description of the work, let us summarize a few attractive features in the PSM approach, which may be relevant for many astrophysical applications.

(i) The PSM begins with solutions from deformed mean-field models and ends up with shell-model diagonalization in the laboratory frame like the spherical shell model. Therefore, the PSM bridges the two groups of important nuclear structure models, namely, the deformed mean-field approach and the conventional shell model, and takes the advantages of both. On the one hand, as a shell model method, the PSM can be applied to study any (super-) heavy, (super-) deformed nuclei without a size limitation. On the other hand, unlike the mean-field models, the PSM wave functions contain correlations beyond the mean fields and the states are written in the laboratory frame having definite quantum numbers such as angular-momentum, particle-number, and parity.

(ii) Since the PSM employs deformed bases, the dimension of the shell-model diagonalization is small (usually about $10^2 \sim 10^4$). Therefore, state-by-state evaluations of nuclear matrix elements for GT transition are computationally feasible for heavy, deformed nuclei. Besides, GT transitions for highly-excited states are calculated directly with the resulting wave functions from diagonalization and the shell-model computation can be much facilitated by employing the modern Pfaffian algorithm [34–38]. Therefore, no approximations such as the Brink-Axel hypothesis are needed for highly-excited states. This feature is important because GT transition rates of highly excited states of heavy nuclei are crucial nuclear inputs for many astrophysical processes.

(iii) The calculation of forbidden transitions involves nuclear transitions between different harmonic oscillator shells and thus requires multishell model spaces. Such calculations are not feasible for most of the conventional shell models working in one-major shell bases. The PSM is a multishell shell model. This feature is desired particularly when forbidden transitions are dominated.

(iv) Nuclear isomeric states play special roles in nuclear physics and astrophysics [39]. The relatively long half-lives of these isomers could change significantly the elemental abundances produced in nucleosynthesis. In some cases, an isomer with long lifetime can change the paths of reaction and lead to a different set of elemental abundances [40]. The PSM has been shown to be a successful model for describing nuclear isomers [41–44].

In this paper, we show the PSM application for GT transitions in heavy, deformed nuclei by taking an example of calculated rates from the even-even nucleus ^{168}Dy to the odd-odd nucleus ^{168}Ho, and demonstrate that considerable strengths show up in the excited states. The paper is organized as follows. In Sec. 2, we will introduce briefly the general formalism of the PSM for the GT calculation. The spectra of ^{168}Dy and ^{168}Ho and the Gamow-Teller transition strengths for the β^- decay between them will be discussed in Sec. 3. Finally, the paper is summarized and an outlook on future applications and developments is given in Sec. 4.

2 Theoretical Framework

The PSM works with the following scheme. It begins with the deformed Nilsson single particle basis [45], with pairing correlations incorporated into the basis by a BCS calculation for the Nilsson states. The Nilsson-BCS calculation defines a deformed quasiparticle (qp) basis. The the angular-momentum (and if necessary, also particle-number, parity) projection is performed on the qp basis to form a shell mdoel space in the laboratory frame. Finally a two-body Hamiltonian is diagonalized in this projected space [24]. Three (four) major harmonic-oscillator shells are usually taken into account in calculations of energy spectra and electromagnetical transitions for heavy (superheavy and superdeformed) nuclei for both neutrons and protons. Let us use $a^\dagger_\nu, a^\dagger_\pi$ (a_ν, a_π) to denote neutron and proton qp creation (annihilation) operators associated with the deformed qp vacuum $|\Phi\rangle$. The multi-qp configurations are given for even-even and odd-odd nuclei as follows:

$$\begin{aligned} &\text{e-e: } \Big\{ |\Phi\rangle,\ a^\dagger_{\nu_i}a^\dagger_{\nu_j}|\Phi\rangle,\ a^\dagger_{\pi_i}a^\dagger_{\pi_j}|\Phi\rangle,\ a^\dagger_{\nu_i}a^\dagger_{\nu_j}a^\dagger_{\pi_k}a^\dagger_{\pi_l}|\Phi\rangle \Big\}, \\ &\text{o-o: } \Big\{ a^\dagger_{\nu_i}a^\dagger_{\pi_j}|\Phi\rangle \Big\}. \end{aligned} \tag{1}$$

It is noted that the PSM works with multiple harmonic-oscillator shells for both neutrons and protons. That is to say, the indices ν (for neutrons) and π (for protons) in Eq. (1) are general; for example, a 2-qp state can be of positive parity if both quasiparticles i and j are from the major N-shells that differ in N by $\Delta N = 0, 2, \ldots$, or of negative parity if i and j are from those N-shells that differ by $\Delta N = 1, 3, \ldots$.

The PSM wave function is a linear combination of the projected states

$$|\Psi^\omega_{IM}\rangle = \sum_{K\kappa} f^\omega_{IK_\kappa} \hat{P}^I_{MK}|\Phi_\kappa\rangle, \tag{2}$$

where $|\Phi_\kappa\rangle$ is the κ-th qp-state in Eq. (1). $\hat{P}^I_{MK}$ is the angular momentum projection operator [46]

$$\hat{P}^I_{MK} = \frac{2I+1}{8\pi^2}\int d\Omega D^I_{MK}(\Omega)\hat{R}(\Omega), \tag{3}$$

with D^I_{MK} being the D-function [47], $\hat{R}$ the rotation operator, and Ω the Euler angles. $f^\omega_{IK_\kappa}$ in (2) are obtained by solving the eigenvalue equation:

$$\sum_{K'\kappa'}\Big(H^I_{K\kappa,K'\kappa'} - E^\omega_I N^I_{K\kappa,K'\kappa'}\Big)f^\omega_{IK'_{\kappa'}} = 0, \tag{4}$$

where $H^I_{K\kappa,K'\kappa'}$ and $N^I_{K\kappa,K'\kappa'}$ are respectively the projected matrix elements of the Hamiltonian and the norm

$$H^I_{K\kappa,K'\kappa'} = \langle\Phi_\kappa|\hat{H}\hat{P}^I_{KK'}|\Phi_{\kappa'}\rangle, \quad N^I_{K\kappa,K'\kappa'} = \langle\Phi_\kappa|\hat{P}^I_{KK'}|\Phi_{\kappa'}\rangle. \tag{5}$$

In Eqs. (2) and (4), we use ω to label different excited states having a same angular momentum I.

The large single-particle space employed in the PSM ensures that the collective motion and the cross-shell interplay are considered microscopically. However, the shell model dimension in Eq. (2) is small, which means that each configuration in Eq. (1) is a complex combination of spherical shell model basis states. Although the dimension where the final diagonalization is carried out is small, it is huge in terms of the original shell model configurations. That is to say, the shell-model space is truncated efficiently in the PSM framework.

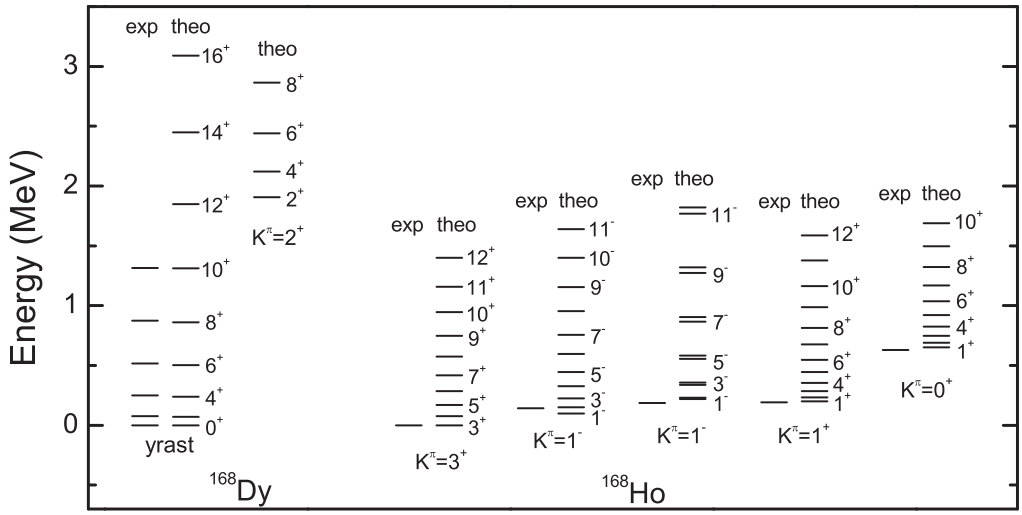

Figure 1. The calculated energy levels of ^{168}Dy and ^{168}Ho, as compared with the experimental data taken from Ref. [56].

The PSM Hamiltonian in the present work consists of the separable forces

$$\hat{H} = \hat{H}_0 + \hat{H}_{\rm QP} + \hat{H}_{\rm GT}, \tag{6}$$

which represent different kinds of correlations among valence nucleons. It has the single-particle terms $\hat{H}_0$, the quadrupole+pairing force $\hat{H}_{\rm QP}$, and the Gamow-Teller force of the charge-exchange terms $\hat{H}_{\rm GT}$. $\hat{H}_0$ is the spherical single-particle term including properly the spin-orbit force. The second force, $\hat{H}_{\rm QP}$, contains three terms [24]

$$\hat{H}_{\rm QP} = -\frac{1}{2}\chi_{\rm QQ}\sum_{\mu}\hat{Q}^{\dagger}_{2\mu}\hat{Q}_{2\mu} - G_M\hat{P}^{\dagger}\hat{P} - G_Q\sum_{\mu}\hat{P}^{\dagger}_{2\mu}\hat{P}_{2\mu}, \tag{7}$$

which correspond to the quadrupole-quadrupole interaction, the monopole-pairing interaction, and the quadrupole-pairing interactions, respectively. The quadrupole+pairing force has been known to take care of basic correlations in nuclear structure, and it has been shown [48] that these interactions simulate the essence of the most important correlations in nuclei, so that any realistic forces have to contain at least these basic components implicitly in order to work successfully in the structure calculations. The strength of the quadrupole-quadrupole term $\chi_{\rm QQ}$ is determined in a self-consistent manner so that it would give the empirical deformation of the basis as predicted in mean-field calculations [24]. The monopole-pairing strength is taken to be the form $G_M = [G_1 \mp G_2(N-Z)/A]/A$, where "+" ("−") is for protons (neutrons), and N, Z, and A are the neutron number, proton number, and mass number, respectively. G_1 and G_2 are the coupling constants adjusted to yield the experimental odd-even staggering of nuclear binding energy in the corresponding nuclear mass region. In this paper, we adopted $G_1 = 20.12$ and $G_2 = 13.13$ as in Ref. [25]. The quadrupole-pairing strength is taken, as usual, to be about 20% of G_M for rare-earth nuclei [24, 25]. It has been shown in many previous publications that such a set of interaction can reasonably well describe nuclear structure properties.

The last force, $\hat{H}_{\rm GT}$ in Eq. (6), is the Gamow-Teller two-body force

$$\begin{aligned}\hat{H}_{\rm GT} = &+ 2\chi_{\rm GT}\sum_{\mu}\hat{\beta}^{-}_{1\mu}(-1)^{\mu}\hat{\beta}^{+}_{1-\mu} \\ &- 2\kappa_{\rm GT}\sum_{\mu}\hat{\Gamma}^{-}_{1\mu}(-1)^{\mu}\hat{\Gamma}^{+}_{1-\mu}.\end{aligned} \tag{8}$$

This is a charge-dependent separable interaction with both particle-hole (ph) and particle-particle (pp) channels, which act between protons and neutrons. Such type of force has been used by many authors in the study of single- and double-β decay [17, 49–52]. The ph and pp interactions are repulsive and attractive, respectively, if we take positive values for the strength parameters $\chi_{\rm GT}$ and $\kappa_{\rm GT}$. The pp interaction, which was introduced originally by Kuz'min and Soloviev [49], is a neutron-proton pairing force in the $J^{\pi} = 1^{+}$ channel. In this work, we adopt the interaction strengths as those in Ref. [49]

$$\chi_{\rm GT} = 23/A, \qquad \kappa_{\rm GT} = 7.5/A. \tag{9}$$

The one-body operators in Eq. (8) are as follows

$$\hat{\beta}^{-}_{1\mu} = \sum_{\pi,\nu}\langle\pi|\sigma_{\mu}\tau_{-}|\nu\rangle c^{\dagger}_{\pi}c_{\nu}, \qquad \hat{\beta}^{+}_{1\mu} = (-)^{\mu}(\hat{\beta}^{-}_{1-\mu})^{\dagger}, \tag{10}$$

$$\hat{\Gamma}^{-}_{1\mu} = \sum_{\pi,\nu}\langle\pi|\sigma_{\mu}\tau_{-}|\nu\rangle c^{\dagger}_{\pi}c^{\dagger}_{\bar{\nu}}, \qquad \hat{\Gamma}^{+}_{1\mu} = (-)^{\mu}(\hat{\Gamma}^{-}_{1-\mu})^{\dagger}. \tag{11}$$

where σ and τ are the Pauli spin operator and the isospin operator, respectively. It is mentioned here that the Hamiltonian in Eq. (6) may need to be extended when specific transition processes are studied. For example, the spin-dipole force would be necessary when calculating first-forbidden transitions [50].

The probability of Gamow-Teller transition from an initial state ω of spin I_i to a final state ω' of spin I_f is defined as

$$B({\rm GT}, I^{\omega}_{i} \to I^{\omega'}_{f}) = \frac{2I_f + 1}{2I_i + 1}\left|\langle\Psi^{\omega'}_{I_f}\|\hat{\beta}^{\pm}\|\Psi^{\omega}_{I_i}\rangle\right|^2, \tag{12}$$

which corresponds to experimental B(GT) values measured directly by the CE reactions or indirectly by the β-decay experiments through

$$ft = \frac{6163.4}{\left(\frac{g_A}{g_V}\right)^2_{\rm eff}B({\rm GT})}, \tag{13}$$

where ft is the comparative half-life, and the coupling constants [53] are adopted as

$$\left(\frac{g_A}{g_V}\right)_{\rm eff} = 0.74\frac{g_A}{g_V}, \qquad \frac{g_A}{g_V} = -1.26. \tag{14}$$

In the present calculation, we assume the axial symmetry in the deformed basis for the mother and daughter nuclei. Then D^{I}_{MK} in Eq. (3) reduces to the small d-function and the three dimensions in Ω

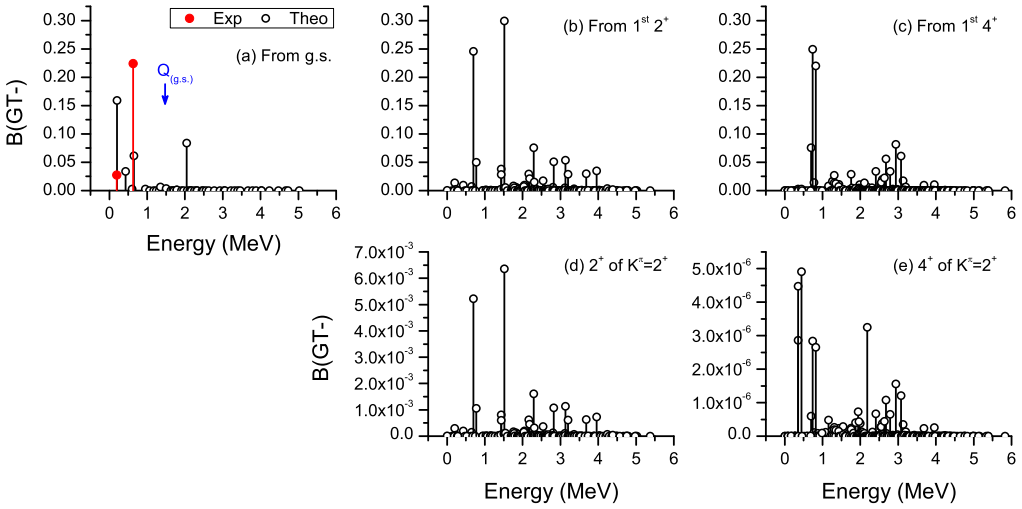

Figure 2. (Color online) The calculated GT transition strength for the β^- decay of ^{168}Dy as a function of the excitation energies for ^{168}Ho, as compared with the data extracted from Ref. [56]. See the text for details.

reduce to one. The following symmetry relations

$$H^I_{K\kappa,K'\kappa'} = H^I_{K'\kappa',K\kappa}, \quad N^I_{K\kappa,K'\kappa'} = N^I_{K'\kappa',K\kappa} \tag{15}$$

$$\langle\Phi_{\kappa'}|\hat{\beta}^{\pm}_{1\mu}\hat{R}(\beta)|\Phi_{\kappa}\rangle = (-)^{K_\kappa - K'_{\kappa'}} \sum_{\mu'} d^1_{\mu'-\mu}(\beta)\langle\Phi_{\kappa}|\hat{\beta}^{\mp}_{1\mu'}\hat{R}(\beta)|\Phi_{\kappa'}\rangle \tag{16}$$

$$\langle\Psi_{I_f}||\hat{\beta}^{\pm}||\Psi_{I_i}\rangle = (-)^{I_f - I_i}\sqrt{\frac{2I_i+1}{2I_f+1}}\langle\Psi_{I_i}||\hat{\beta}^{\mp}||\Psi_{I_f}\rangle \tag{17}$$

together with the Ikeda sum-rule can then be used for testing the codes and checking numerical correctness [32].

3 Results and Discussion

The standard Nilsson scheme [45] is used for generating the deformed basis. In the present work, the Nilsson parameters to generate the basis are taken from Refs. [54, 55]. Three major shells, $N = 3, 4, 5$ ($N = 4, 5, 6$), are adopted for protons (neutrons). The quadrupole and hexadecapole deformation parameters are taken as $\varepsilon_2 = 0.275, \varepsilon_4 = 0.070$ for ^{168}Dy and $\varepsilon_2 = 0.275, \varepsilon_4 = 0.030$ for ^{168}Ho, respectively.

Figure 1 shows the calculated energy levels of ^{168}Dy and ^{168}Ho, which are compared with the experimental data from Ref. [56]. It is seen that the known energy levels of the yrast band of ^{168}Dy is well reproduced by the calculation. In addition, an excited 2^+ band is predicted as an example of 2-qp configurations, and has the configuration of $\nu 1/2^-[521] \otimes \nu 5/2^-[512]$. GT transitions related to this 2^+ band will also be discussed below. For ^{168}Ho, only a few states are experimentally known so far. The calculation shows that the spin and parity of the ground state (g.s.) in ^{168}Ho, the 3^+ state, are reproduced correctly. The main configuration of this 3^+ state is $\nu 1/2^-[521] \otimes \pi 7/2^-[523]$. Above the g.s., there are two 1^- states at the excitation energies 143 keV and 187 keV, respectively. The energies

of these two 1^- states are nicely reproduced. The configuration of the lower 1^- state is found to be $\nu 1/2^-[521]\otimes\pi 3/2^+[411]$ and $K^\pi = 1^-$, while the higher one is $\nu 1/2^-[521]\otimes\pi 1/2^+[411]$ and $K^\pi = 1^-$. Three rotational bands based on the g.s. and the two 1^- states are shown Fig. 1, and a strong signature dependence is found for the higher 1^- band.

Experimentally, GT transitions from the g.s. of ^{168}Dy to two 1^+ states of ^{168}Ho have been measured [56]. The lower positive-parity 1^+ state at 192 keV is a 108-ns isomer. It is seen from Fig. 1 that the energies of both 1^+ states in ^{168}Ho are reproduced well. The configuration of the lower 1^+ state is found to be $\nu 5/2^-[512]\otimes\pi 7/2^-[523]$ and $K^\pi = 1^+$, while that of the higher is $\nu 7/2^+[633]\otimes\pi 7/2^+[404]$ and $K^\pi = 0^-$. Thus the above results indicate that the present PSM calculation can describe the relevant low-lying levels of the mother and daughter nucleus reasonably well.

Figure 2 shows the calculated GT transition strength B(GT) of the β^- decay from ^{168}Dy to ^{168}Ho. B(GT) of the yrast band (states in the $K^\pi = 0^+$ band) and the excited 2^+ band for ^{168}Dy are shown in the upper and lower plots, respectively, as a function of excitation energies of ^{168}Ho. The known experimental B(GT) values from the g.s. of ^{168}Dy to the two 1^+ states of ^{168}Ho are extracted from Ref. [56] by using Eq. (13), and shown in Fig. 2 for comparison. It is seen that the PSM can reproduce the data with the correct order of magnitude. In addition, a strong GT transition is predicted at about 2 MeV. As seen from Fig. 2(a), the calculation predicts many small GT strengths up to 5 MeV, beyond which states are truncated out from the present configuration space in Eq. (1). Clearly, more transitions should exist in the highly-excited region if one enlarges the configuration space by including multi-qp states.

Little about GT transitions from excited states is known experimentally, because excited states decay normally through electromagnetic transitions. However, in stellar environments, nuclei are exposed to high temperatures, and thermally-populated excited i-th state in nuclei would have a certain population probability according to the Boltzmann factor and the statistical weight

$$p_i = \frac{(2I_i + 1)e^{-E_i/kT}}{\sum_m (2I_m + 1)e^{-E_m/kT}}. \tag{18}$$

The GT transition information from excited states thus becomes important in stellar environments. Figure 2(b) shows the calculated B(GT) rates from the first 2^+ state (the first excited state in the yrast band) of ^{168}Dy. Larger fragmentation of the B(GT) is seen when compared with the rates of the g.s., which is partly due to the larger state-space (i.e., nuclear states with nonzero angular momentum contain different varieties of the K configurations) and the corresponding configuration mixture. The same situation happens for the first 4^+ state (the second excited state in the yrast band), as seen from the plot (c). In this plot, the GT strengths seem to peak at about 3 MeV. Again, the disappearance of the strength at higher excitation energies is due to the truncation effect.

From the above discussion it could be concluded that the GT strength distributions depend sensitively on the size of the state-space (i.e. configuration mixture). In the lower row of the plots in Fig. 2, we show the calculated GT transition rates from the $K^\pi = 2^+$ 2-qp band of the mother nucleus ^{168}Dy. As seen from Fig. 2(d), the GT strength from the 2^+ state of the 2^+ band has a similar distribution pattern with the one of the first 2^+ state of the yrast band in Fig. 2(b), but is by about two orders of magnitude weaker (Note the different scales between Fig. 2(b) and (d)). Even more fragmented, but weak GT transitions from the 4^+ state of the 2^+ band are predicted, as seen in Fig. 2(e).

4 Summary and future works

In summary, a shell-model method for calculating Gamow-Teller transition rates for heavy, deformed nuclei has been proposed by using the concept of the Projected Shell Model (PSM). The shell-model

basis of the PSM is constructed by superimposing angular-momentum-projected multi-quasiparticle (qp) configurations, and nuclear wave functions are obtained by diagonalizing the two-body interactions in these projected states. We have shown that with this method, it is then possible to perform a state-by-state calculation of the nuclear matrix elements for β-decay in heavy, deformed nuclei. We have taken β^- decay of ^{168}Dy to ^{168}Ho as an example, and shown that the PSM can well describe the spectrum of the relevant nuclei, and can reproduce the available experimental B(GT) from the ground state of the mother nucleus to the low-lying states of the daughter nucleus. Furthermore, comparably strong GT transitions form the excited states are predicted to occur. The GT transitions from excited states have been found to be sensitively dependent of the size of model space. Thus the configuration mixture is very important for predicting B(GT) of excited states.

Since the distribution of GT transition depends on the model space, higher-order qp excitation modes are being considered in our model, which requires enlargement of our shell-model space by including higher-order multi-qp states in the configuration space. Particle-number projection for removing possible spurious states associated with particle number violation of the BCS method, as well as the spin-dipole force for calculating the first-forbidden GT transitions are also planned as future works.

Acknowledgements

Research at SJTU was supported by the National Natural Science Foundation of China (Nos. 11575112, 11135005), by the 973 Program of China (No. 2013CB834401), and by the Open Project Program of the State Key Laboratory of Theoretical Physics, Institute of Theoretical Physics, Chinese Academy of Sciences, China (No. Y5KF141CJ1).

References

[1] G. M. Fuller, W. A. Fowler, and M. J. Newman, Astrophys. J. Suppl. **42**, 447 (1980).
[2] G. M. Fuller, W. A. Fowler, and M. J. Newman, Astrophys. J. **252**, 715 (1982).
[3] G. M. Fuller, W. A. Fowler, and M. J. Newman, Astrophys. J. Suppl. **48**, 279 (1982).
[4] G. M. Fuller, W. A. Fowler, and M. J. Newman, Astrophys. J. **293**, 1 (1985).
[5] K. Langanke and G. Martínez-pinedo, Rev. Mod. Phys. **75**, 819 (2003).
[6] F. T. Avignone III, S. R. Elliott and J. Engel, Rev. Mod. Phys. **80**, 481 (2008).
[7] C. J. Guess *et al*., Phys. Rev. C **83**, 064318 (2011).
[8] H.-Th. Janka, K. Langanke, A. Marek, G. Martínez-Pinedo, B. Müller, Phys. Rep. **442**, 38 (2007).
[9] A. L. Cole *et al*., Phys. Rev. C **86**, 015809 (2012).
[10] D. M. Brink, Ph.D. thesis, Oxford University, 1955.
[11] P. Axel, Phys. Rev. **126**, 671 (1962).
[12] G. W. Misch, G. M. Fuller, and B. A. Brown, Phys. Rev. C **90**, 065808 (2014).
[13] Y. Fujita, B. Rubio, and W. Gelletly, Prog. Part. Nucl. Phys. **66**, 549 (2011).
[14] F. Osterfeld, Rev. Mod. Phys., **64**, 491 (1992).
[15] N. Ryezayeva *et al.*, Phys. Lett. B **639**, 623 (2006).
[16] S. Rakers *et al.*, NIM A **481**, 253 (2002).
[17] P. Sarriguren, Phys. Rev. C **87**, 045801 (2013).
[18] E. Caurier, G. Martínez-Pinedo, F. Nowacki, A. Poves and A. P. Zuker, Rev. Mod. Phys. **77**, 427 (2005).
[19] M. B. Aufderheide, S. D. Bloom, D. A. Resler and G. J. Mathews, Phys. Rev. C **47**, 2961 (1993).

[20] B. H. Wildenthal, Prog. Part. Nucl. Phys. **11**, 5 (1984).
[21] B. A. Brown and B. H. Wildenthal, At. Data Nucl. Data Tables **33**, 347 (1985).
[22] T. Oda *et al*., At. Data Nucl. Data Tables **56**, 231 (1994).
[23] K. Langanke and G. Martínez-Pinedo, At. Data Nucl. Data Tables **79**, 1 (2001).
[24] K. Hara and Y. Sun, Int. J. Mod. Phys. E **4**, 637 (1995).
[25] Y. Sun and D. H. Feng, Phys. Rep. **264**, 375 (1996).
[26] Y. Sun, J.-y. Zhang, and M. Guidry, Phys. Rev. Lett. **78**, 2321 (1997).
[27] F. Al-Khudair, G.-L. Long, and Y. Sun, Phys. Rev. C **79**, 034320 (2009).
[28] B.-A. Bian, Y. Sun, and Y.-C. Yang, Phys. Rev. C **89**, 014317 (2014).
[29] Y.-C. Yang, Y. Sun, S.-J. Zhu, M. Guidry, and C.-L. Wu, J. Phys. G: Nucl. Part. Phys. **37** 085110 (2010).
[30] Y.-X. Liu, Y. Sun, X.-H. Zhou, Y.-H. Zhang, S.-Y. Yu, Y.-C. Yang, and H. Jin, Nucl. Phys. A **858**, 11 (2011).
[31] Y. Sun, Y.-C. Yang, H. Jin, K. Kaneko, and S. Tazaki, Phys. Rev. C **85**, 054307 (2012).
[32] Z.-C. Gao, Y. Sun, and Y.-S. Chen, Phys. Rev. C **74**, 054303 (2006).
[33] L.-J. Wang and Y. Sun, to be published.
[34] L. M. Robledo, Phys. Rev. C **79**, 021302(R) (2009).
[35] G. F. Bertsch and L. M. Robledo, Phys. Rev. Lett. **108**, 042505 (2012).
[36] T. Mizusaki, M. Oi, F. Q. Chen, and Y. Sun, Phys. Lett. B **725**, 175 (2013).
[37] Q.-L. Hu, Z.-C. Gao, and Y. S. Chen, Phys. Lett. B **734**, 162 (2014).
[38] L.-J. Wang, F.-Q. Chen, T. Mizusaki, M. Oi, and Y. Sun, Phys. Rev. C **90**, 011303(R) (2014).
[39] A. Aprahamian and Y. Sun, Nature Phys. **1**, 81 (2005).
[40] Y. Sun, M. Wiescher, A. Aprahamian, and J. Fisker, Nucl. Phys. A **758**, 765 (2005).
[41] Y. Sun, X.-R. Zhou, G.-L. Long, E.-G. Zhao, and P. M. Walker, Phys. Lett. B **589**, 83 (2004).
[42] Y. Sun, M. Wiescher, A. Aprahamian, and J. Fisker, AIP Conf. Proc. **819**, 196 (2006).
[43] Y. Sun, AIP Conf. Proc. **819**, 30 (2006).
[44] R.-D. Herzberg *et al*., Nature **442**, 896 (2006).
[45] S. G. Nilsson *et al*., Nucl. Phys. A **131**, 1 (1969).
[46] P. Ring and P. Schuck, *The nuclear many-body problem* (Springer Verlag, Berlin, 2004).
[47] D. A. Varshalovich, A. N. Moskalev, and V. K. Khersonskii, *Quantum theory of angular momentum* (World Scientific, Sigapore, 1988).
[48] M. Dufour and A. P. Zuker, Phys. Rev. C **54**, 1641 (1996).
[49] V. A. Kuz'min and V. G. Soloviev, Nucl. Phys. A **486**, 118 (1988).
[50] H. Homma, E. Bender, M. Hirsch, K. Muto, H. V. Klapdor-Kleingrothaus, and T. Oda, Phys. Rev. C **54**, 2972 (1996).
[51] J. Suhonen and O. Civitarese, Phys. Rep. **300**, 123 (1998).
[52] O. Moreno *et al*., Prog. Part. Nucl. Phys. **57**, 254 (2006).
[53] K. Langanke and G. Martínez-Pinedo, Nucl. Phys. A **673**, 481 (2000).
[54] F. Dickmann and K. Dietrich, Z. Phys. **263**, 211 (1973).
[55] T. Bengtsson and I. Ragnarsson, Nucl. Phys. A **436**, 14 (1985).
[56] C. M. Baglin, Nuclear Data Sheets, **111**, 1807 (2010).